

Induction of Secondary Metabolites from the Marine-Derived Fungus *Aspergillus versicolor* through Co-cultivation with *Bacillus subtilis*

Authors

Nada M. Abdel-Wahab^{1,2*}, Sebastian Scharf^{1*}, Ferhat C. Özkaya¹, Tibor Kurtán³, Attila Mándi³, Mostafa A. Fouad², Mohamed S. Kamel^{2,4}, Werner E. G. Müller⁵, Rainer Kalscheuer¹, Wenhan Lin⁶, Georgios Daletos¹, Weaam Ebrahim^{1,7}, Zhen Liu¹, Peter Proksch¹

Affiliations

- 1 Institut für Pharmazeutische Biologie und Biotechnologie, Heinrich-Heine-Universität Düsseldorf, Düsseldorf, Germany
- 2 Department of Pharmacognosy, Faculty of Pharmacy, Minia University, Minia, Egypt
- 3 Department of Organic Chemistry, University of Debrecen, Debrecen, Hungary
- 4 Department of Pharmacognosy, Faculty of Pharmacy, Deraya University, New Minia, Egypt
- 5 Institut für Physiologische Chemie, Universitätsmedizin der Johannes-Gutenberg-Universität Mainz, Mainz, Germany
- 6 State Key Laboratory of Natural and Biomimetic Drugs, Peking University, Beijing, China
- 7 Department of Pharmacognosy, Faculty of Pharmacy, Mansoura University, Mansoura, Egypt

Key words

sponge-derived fungus, *Aspergillus versicolor*, cyclic pentapeptide, co-culture, ECD calculations, cytotoxicity, antibacterial activity

received August 24, 2018

revised January 9, 2019

accepted January 13, 2019

Bibliography

DOI <https://doi.org/10.1055/a-0835-2332>

Published online January 30, 2019 | *Planta Med* 2019; 85: 503–512 © Georg Thieme Verlag KG Stuttgart · New York | ISSN 0032-0943

Correspondence

Weaam Ebrahim

Institut für Pharmazeutische Biologie und Biotechnologie, Heinrich-Heine-Universität Düsseldorf

Universitätsstr. 1, 40225 Düsseldorf, Germany

Phone: + 49 21 18 11 41 63, Fax: + 49 21 18 11 19 23

weaam.ebrahim@uni-duesseldorf.de

Correspondence

Zhen Liu

Institut für Pharmazeutische Biologie und Biotechnologie, Heinrich-Heine-Universität Düsseldorf

Universitätsstr. 1, 40225 Düsseldorf, Germany

Phone: + 49 21 18 11 59 79, Fax: + 49 21 18 11 19 23

zhenfeizi@sina.com

Correspondence


Peter Proksch

Institut für Pharmazeutische Biologie und Biotechnologie, Heinrich-Heine-Universität Düsseldorf

Universitätsstr. 1, 40225 Düsseldorf, Germany

Phone: + 49 21 18 11 41 63, Fax: + 49 21 18 11 19 23

proksch@uni-duesseldorf.de

 Supporting information available online at <http://www.thieme-connect.de/products>

ABSTRACT

A new cyclic pentapeptide, cotteslosin C (**1**), a new aflaquinolone, 22-epi-aflaquinolone B (**3**), and two new anthraquinones (**9** and **10**), along with thirty known compounds (**2**, **4–8**, **11–34**) were isolated from a co-culture of the sponge-associated fungus *Aspergillus versicolor* with *Bacillus subtilis*. The new metabolites were only detected in the co-culture extract, but not when the fungus was grown under axenic conditions. Furthermore, the co-culture extract exhibited an enhanced accumulation of the known constituents versicolorin B (**14**), averufin (**16**), and sterigmatocystin (**19**) by factors of 1.5, 2.0, and 4.7, respectively, compared to the axenic fungal culture. The structures of the isolated compounds were elucidated on the basis of 1D and 2D NMR spectra and mass spectrometry as well as by comparison with literature data. The absolute configuration of compounds **3**, **9**, and **10** was determined by ECD (electronic circular dichroism) analysis aided by TDDFT-ECD (time-dependent density functional theory electronic circular dichroism) calculations. Compounds **15**, **18–21**, and **26** exhibited strong to moderate cytotoxic activity

* These authors contributed equally to this work.

against the mouse lymphoma cell line L5178Y, with IC₅₀ values ranging from 2.0 to 21.2 μM, while compounds **14**, **16**, **31**, **32**, and **33** displayed moderate inhibitory activities

against several gram-positive bacteria, with MIC values ranging from 12.5 to 50 μM.

Introduction

Sponge-associated fungi have repeatedly been shown to be promising sources for drug discovery [1]. These fungi are able to synthesize structurally remarkable compounds such as the rare *N*-methylated peptides endolides A and B that were isolated from sponge-associated *Stachylidium* sp. and showed affinity to vasopressin and serotonin receptors [2]. Furthermore, investigation of the sponge-derived fungus *Aspergillus violaceofuscus* led to the isolation of three new cyclopeptides, including the cyclic tetrapeptide violaceotide A, an aspochracin-type cyclic tripeptide sclerotiotide L, and a new diketopiperazine dimer, with both violaceotide A and the new diketopiperazine dimer exhibiting anti-inflammatory activity [3]. However, the rediscovery rate of known compounds from microorganisms including sponge-associated fungi is a serious problem in natural product chemistry, as gene clusters responsible for biosynthesis of secondary metabolites often remain silent under axenic culture conditions. Thus, only a fraction of microbial metabolites compared to the genetic potential of an organism can usually be detected in fungal extracts [4]. Besides, microorganisms live as part of microbial communities where they are submitted to competition for nutrients with other eukaryotic and prokaryotic microbes. Mimicking the natural microbial ecosystem is the main purpose of co-culture strategies, thus aiming at an induction of silent biosynthetic gene clusters [5]. Applying co-culture techniques has repeatedly led to the discovery of new bioactive compounds that were not detected in axenic cultures. In our previous study, two new sesquiterpenoids, pestabacillins A and B, which were not detected in an axenic culture of *Pestalotiopsis* sp., were isolated from the co-culture of *Pestalotiopsis* sp. and *Bacillus subtilis* [6]. In addition, mixed fermentation of the fungus *Aspergillus austroafricanus* with either *B. subtilis* or *Streptomyces lividans* on solid rice medium led to an enhanced accumulation of several diphenyl ether derivatives, including the new compound austramide, compared to axenic fungal cultures [7]. Moreover, several cryptic metabolites, including the two new compounds aspvancins A and B, were isolated from the co-culture of the endophytic fungus *Aspergillus versicolor* with the bacterium *B. subtilis* but were likewise lacking in axenic fungal cultures [8].

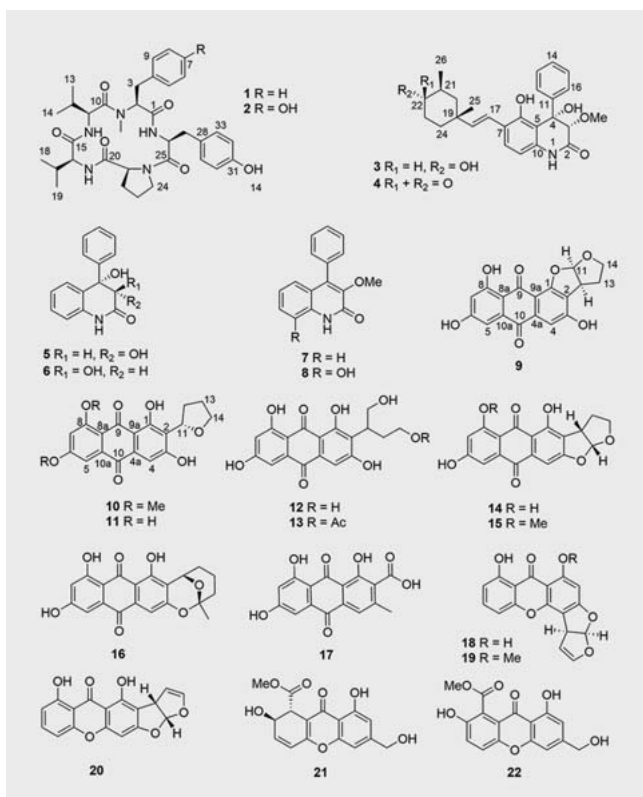
In the present study, a co-culture experiment of the sponge-associated fungus *A. versicolor* with the bacterium *B. subtilis* was conducted. Several metabolites, including sterigmatocystin, versicolorin B, and averufin, exhibited an increased accumulation in the fungal-bacterial co-culture compared to the axenic fungal culture. Furthermore, the co-culture yielded four new metabolites (**1**, **3**, **9**, and **10**) that were not detected in the axenic fungal culture. Herein, we report the structure elucidation of the new compounds in addition to the biological activities of the isolated metabolites (► **Figs. 1** and **2**).

Results and Discussion

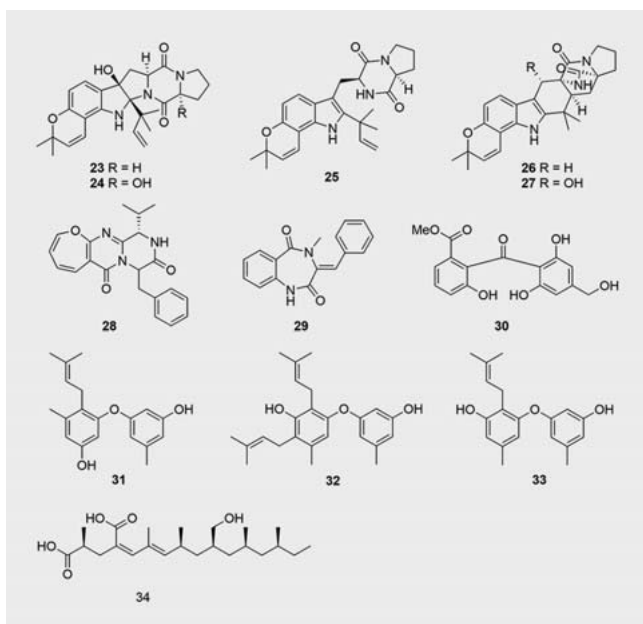
Axenic cultures of *A. versicolor* or *B. subtilis* and co-cultures were grown on solid rice medium under static conditions. When reaching the stationary phase of growth, EtOAc was added, followed by filtration and extraction. The obtained extracts were analyzed by analytical HPLC to monitor the chromatographic patterns prior to the isolation procedure. Comparison of axenic fungal or bacterial cultures with the mixed fungal-bacterial cultures showed the striking of compounds **14**, **16**, and **19** in the mixed cultures in addition to the induction of four new metabolites (**1**, **3**, **9**, and **10**) that were not detected in the axenic fungal or bacterial cultures.

Compound **1** was obtained as a dark amorphous solid. Its molecular formula was deduced as C₃₄H₄₅N₅O₆ from HRESIMS, implying 15 degrees of unsaturation. Examination of the ¹H-NMR, COSY, HSQC, and HMBC data of **1** revealed its peptide nature and showed its close similarity to the co-isolated known peptide cotteslosin A (**2**), which was previously obtained from a marine-derived strain of *A. versicolor* [9]. Interpretation of the ¹H-NMR spectrum (► **Table 1**) of **1** showed the presence of only one phenolic OH group at δ_H 9.24 instead of two phenolic OH groups as in cotteslosin A (**2**). Moreover, compound **1** had one 1,4-disubstituted benzene ring and a monosubstituted benzene ring, unlike compound **2**, which features two 1,4-disubstituted benzene rings. Detailed inspection of the 2D NMR spectra of **1** (► **Fig. 3**) confirmed the replacement of *N*-methyl-tyrosine in cotteslosin A (**2**) with *N*-methyl-phenylalanine in compound **1**, accounting for the difference in molecular weight and NMR data between these two compounds. The absolute configurations of the amino acids were determined after acid hydrolysis of **1** followed by Marfey's derivatization method, which indicated that all amino acids were present in the L-form. In conclusion, compound **1** was identified as a new natural product and was given the name cotteslosin C.

The molecular formula of compound **3** was determined to be C₂₆H₃₁NO₅ on the basis of the HRESIMS data. It had UV absorbance maxima at 212, 278, and 324 nm. The ¹H and ¹³C NMR data of compound **3** (► **Table 2**) were similar to those of the previously reported compound aflaquinolone B [10]. Detailed analysis of the 2D NMR spectra of **3** confirmed that these two compounds share the same planar structure (► **Fig. 4**). The obvious difference between **3** and aflaquinolone B was observed in the cyclohexane part of the structure. The ¹H-NMR spectrum of **3** revealed that H-20 is coupled to the neighboring proton H-21 with a large *trans*-diaxial-type coupling constant (13 Hz), implying that H-20 and H-21 should be axially oriented and the methyl group at C-21 is in equatorial orientation, as reported in aflaquinolone B. However, H-22 of **3** showed a large *trans*-diaxial-type coupling constant (10.4 Hz) with H-21, indicating that H-22 is axially oriented and the hydroxy group at C-22 has an equatorial orientation, unlike aflaquinolone B where the C-22 hydroxy group is in the axial orientation. Consequently, the only difference between **3** and aflaquinolone B



► Fig. 1 Structures of compounds 1–22.



► Fig. 2 Structures of compounds 23–34.

nolone B was the orientation of the hydroxy group at C-22. Thus, compound 3 was found to be the new C-22 epimer of aflaquinolone B and was given the trivial name 22-epi-aflaquinolone B. The electronic circular dichroism (ECD) data of 3 showed the same

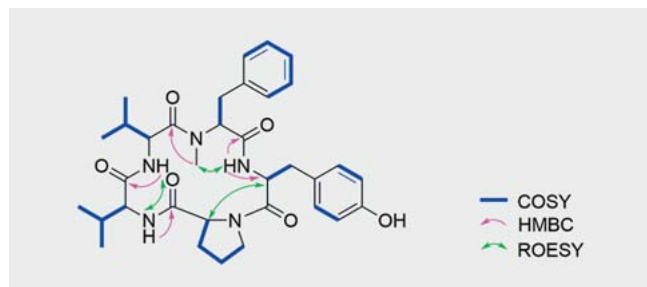
► Table 1 ¹H and ¹³C NMR data of compound 1^a.

Position	δ_C^b	δ_H , m (J in Hz)
1	167.7	
2	61.1, CH	4.22, dd (11.7, 3.2)
2-NMe	30.1, CH ₃	2.69, s
3	33.5, CH ₂	3.31, (overlapped)
		2.75, dd (14.2, 11.8)
4	137.0, C	
5/9	128.9, CH	7.17, d (7.7)
6/8	128.2, CH	7.30, t (7.7)
7	126.3, CH	7.23, t (7.7)
10	170.1, C	
11	52.3, CH	3.57, t (8.1)
11-NH		8.23, d (9.1)
12	29.4, CH	1.70, m
13	18.8, CH ₃	0.35, d (6.7)
14	17.6, CH ₃	0.57, d (6.9)
15	169.1, C	
16	60.9, CH	3.99, m
16-NH		7.30, d (9.4)
17	30.6, CH	1.77, m
18	19.1, CH ₃	0.84, d (6.6)
19	18.7, CH ₃	0.77, d (6.5)
20	169.9, C	
21	60.7, CH	3.99, m
22	31.2, CH ₂	1.90, m
23	21.5, CH ₂	1.73, m
		1.61, m
24	46.0, CH ₂	3.47, m
		3.37, m
25	168.6, C	
26	52.7, CH	4.64, m
26-NH		6.83, d (7.4)
27	37.0, CH ₂	2.95, dd (13.1, 9.5)
		2.81, dd (13.1, 4.5)
28	126.6, C	
29/33	129.8, CH	7.01, d (8.5)
30/32	114.7, CH	6.67, d (8.5)
31	155.4, C	
31-OH		9.24, s

^aMeasured in DMSO-*d*₆ (¹H at 600 MHz and ¹³C at 150 MHz). ^bData were extracted from the HSQC and HMBC spectra

ECD pattern as that of aflaquinolone B [10], indicating that they shared the same absolute configuration at C-3 and C-4 of the dihydroquinoline unit.

Compound 9 was obtained as an orange red powder that exhibited UV maxima at 223, 285, and 437 nm, characteristic of anthraquinone derivatives. The HRESIMS of compound 9 displayed a



► **Fig. 3** Key COSY, HMBC, and NOE correlations of compound **1**.

pseudomolecular ion peak at m/z 341.0654 $[M + H]^+$ in accordance with the molecular formula $C_{18}H_{12}O_7$, with 13 degrees of unsaturation. The NMR data of **9** (► **Table 3**) showed signals attributed to a pentasubstituted anthraquinone moiety. The presence of a fused tetrahydrofuran ring was evident from the COSY spectrum of **9**, which revealed a spin system from the significant downfield shifted dioxymethine proton H-11 (δ_H 6.53) to oxy-methylene protons H₂-14 (δ_H 4.06 and 3.47) through H-12 (δ_H 4.01) and H₂-13 (δ_H 2.16 and 2.10), as well as from the HMBC correlations from H-11 to C-14 (δ_C 66.9), and in turn from H-14 to C-11 (δ_C 113.3) (► **Fig. 5**). These structural features resemble the co-isolated known compound versicolorin B (**14**) [11, 12]. The major difference was that compound **9** had only one chelated OH proton resonance at δ_H 13.31 in contrast to versicolorin B (**14**), which showed signals of two chelated OH protons. This could be explained by the connection of the tetrahydrofuran ring and the anthraquinone moiety at C-1 and C-2 in compound **9**, which was proven by the HMBC correlations from H-11 to C-1 (δ_C 161.7) and C-2 (δ_C 121.3), and from H-12 to C-1, C-2, and C-3 (δ_C 159.3). Hence, compound **9** was elucidated as an isomer of versicolorin B (**14**), which differs from the latter in the position of the fused furan ring. The NOE correlation between H-11 and H-12 suggested a *cis* configuration of these two protons.

To elucidate the absolute configuration of **9**, the solution TDDFT-ECD method was applied on the arbitrarily chosen (11*S*,12*R*) enantiomer [13, 14]. The Merck molecular force field (MMFF) conformational search resulted in 8 geometries in a 21 kJ/mol energy window, which were reoptimized at both the B3LYP/6-31G(d) and CAM-B3LYP/TZVP PCM/MeCN levels. The Boltzmann-weighted ECD spectra of (11*S*,12*R*)-**9** calculated for the low-energy ($\geq 1\%$) DFT conformers at various levels (B3LYP/TZVP, BH&HLYP/TZVP, CAM-B3LYP/TZVP, and PBE0/TZVP), as both sets of conformers gave mirror-image ECD spectra of the experimental curve at all applied combinations of levels (► **Fig. 6**). Furthermore, the low-energy conformers differed only in the orientation of the OH protons (► **Fig. 7**), allowing the unambiguous elucidation of the absolute configuration of **9** as (11*R*,12*S*).

The UV spectrum of compound **10** showed absorption maxima at 223, 287, and 440 nm, suggesting its anthraquinone nature. Investigation of the NMR spectra of compound **10** (► **Table 3**) displayed signals of a pentasubstituted anthraquinone and a saturated furan ring with close structural resemblance to bipolarin (**11**) [15]. The molecular formula of compound **10** was determined to be $C_{20}H_{18}O_7$ by HRESIMS, 28 amu higher than that of bipolarin

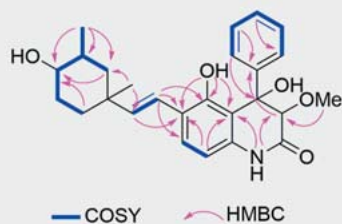
► **Table 2** 1H and ^{13}C NMR data of compound **3**^a.

Position	δ_C^b	δ_H , m (J in Hz)
1-NH		7.36, br s
2	164.9, C	
3	84.1, CH	3.69, br s
4	78.7, C	
5	110.5, C	
6	154.6, C	
7	122.8, C	
8	127.1, CH	7.38, d (8.3)
9	106.7, CH	6.33, d (8.3)
10	133.7, C	
11	137.3, C	
12/16	126.3, CH	7.28, m
13/15	128.9, CH	7.31, m
14	129.2, CH	7.31, m
17	121.5, CH	6.60, d (16.6)
18	137.6, CH	6.14, d (16.6)
19	37.0, C	
20	45.9, CH ₂	1.74, m 1.07, t (13.0)
21	36.1, CH	1.58, m
22	77.0, CH	3.12, ddd (10.4, 10.4, 4.2)
23	31.9, CH ₂	1.78, m 1.51, m
24	36.8, CH ₂	1.82, m 1.37, ddd (13.6, 13.6, 3.4)
25	31.1, CH ₃	1.03, s
26	18.6, CH ₃	0.98, d (6.4)
3-OMe	58.9, CH ₃	3.61, s
4-OH		4.60, s
6-OH		9.04, s

^aMeasured in $CDCl_3$ (1H at 600 MHz and ^{13}C at 150 MHz). ^bData were extracted from the HSQC and HMBC spectra

(**11**). This could be attributed to the presence of two additional aromatic methoxy groups at δ_H 4.02 (s) and 4.01 (s) in the 1H -NMR spectrum of **10** that exhibited HMBC correlations to C-6 (δ_C 165.6) and C-8 (δ_C 163.8), respectively, unlike bipolarin with two hydroxy groups at C-6 and C-8. Therefore, compound **10** was identified as the new compound 6,8-*O*-dimethylbipolarin (► **Fig. 8**).

The same TDDFT-ECD computational protocol as for **9** was applied on the arbitrarily chosen (*R*)-**10** to determine the absolute configuration. DFT reoptimization of the 15 initial MMFF conformers resulted in 8 and 4 low-energy conformers at the B3LYP/6-31G (d) and CAM-B3LYP/TZVP PCM/MeOH levels, respectively. ECD spectra computed at various levels for each set of conformers gave mirror-image agreement with the experimental one, allowing for elucidation of the absolute configuration as (*S*) (► **Fig. 9**).



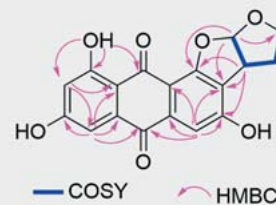
► Fig. 4 Key COSY and HMBC correlations of compound 3.

► Table 3 ¹H and ¹³C NMR data of compounds 9 and 10.

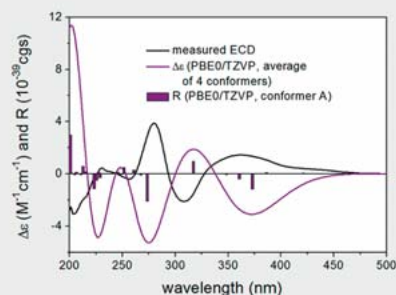
Position	9 ^a		10 ^b	
	δ _C	δ _H , m (J in Hz)	δ _C ^c	δ _H , m (J in Hz)
1	161.7, C		161.8, C	
2	121.3, C		122.3, C	
3	159.3, C		163.2, C	
4	109.2, CH	7.22, s	108.2, CH	7.07, s
4a	134.7, C		133.0, C	
5	107.3, CH	7.02, d (2.3)	105.1, CH	7.36, d (2.5)
6	164.0, C		165.6, C	
7	108.0, CH	6.53, d (2.3)	104.8, CH	6.99, d (2.5)
8	164.3, C		163.8, C	
8a	109.5, C		115.1, C	
9	184.7, C		186.2, C	
9a	107.9, C		110.3, C	
10	181.8, C		182.4, C	
10a	134.5, C		137.8, C	
11	113.3, CH	6.53, d (6.1)	70.0, CH	5.42, dd (8.1, 4.4)
12	42.8, CH	4.01, dd (8.5, 6.1)	34.1, CH	1.94, m
13	30.5, CH ₂	2.16, m 2.10, m	29.7, CH ₂	1.76, m
14	66.9, CH ₂	4.06, dd (8.9, 7.5) 3.47, ddd (12.0, 8.9, 5.1)	62.1, CH ₂	3.66, ddd (10.5, 5.9, 5.9) 3.60, ddd (10.5, 7.1, 5.8)
1-OH				14.11, s
6-OMe			56.5, CH ₃	4.02, s
8-OH		13.31, s		
8-OMe			56.8, CH ₃	4.01, s

^a Measured in DMSO-*d*₆ (¹H at 600 MHz and ¹³C at 150 MHz). ^b Measured in acetone-*d*₆ (¹H at 600 MHz and ¹³C at 150 MHz). ^c Data were extracted from the HSQC and HMBC spectra

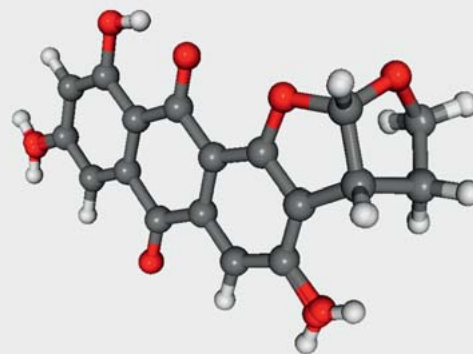
The known compounds were identified as cotteslosin A (2) [9], aflaquinolone A, F, and G (4-6) [10], 3-*O*-methylviridicatin (7) [16], 9-hydroxy-3-methoxyviridicatin (8) [17], bipolarin (11) [15], versiconol (12) [18], versiconol acetate (13) [19], versicolorin B



► Fig. 5 Key COSY and HMBC correlations of compound 9.

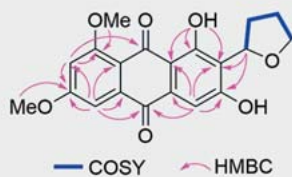


► Fig. 6 Experimental ECD spectrum (black) of 9 in MeCN compared with the Boltzmann-weighted PBE0/TZVP PCM/MeCN ECD spectrum (purple) of (11*S*,12*R*)-9 computed for the four low-energy CAM-B3LYP/TZVP PCM/MeCN conformers. The bars represent the rotational strength values of the lowest energy conformer.

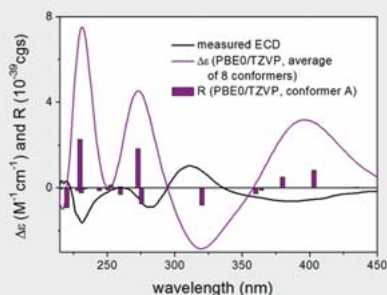


► Fig. 7 Four overlapped solution conformers of (11*S*,12*R*)-9 with Boltzmann populations of 42.8, 39.8, 8.2, and 7.7% indicating that they differ only in the orientation of the OH protons.

(14) [11, 12], 8-*O*-methylversicolorin B (15) [20], averufin (16) [21], endocrocin (17) [22], *O*-demethylsterigmatocystin (18) [23], sterigmatocystin (19) [18], sterigmatin (20) [23], AGI-B4 (21) [24], sydowinin B (22) [25], notoamide D (23) [26], speramide B (24) [27], notoamide E (25) [28], stephacidin A (26) [29], notoamide R (27) [30], protuboxepin B (28) [31], 3,10-dehydrocycloopteine (29) [32], penicillanone (30) [33], diorcinol D (31) [34], diorcinol G (32) [35], diorcinol I (33) [35], and radiclonic acid



► **Fig. 8** Key COSY and HMBC correlations of compound **10**.



► **Fig. 9** Experimental ECD spectrum (black) of **10** in MeOH compared with the Boltzmann-weighted PBE0/TZVP ECD spectrum (purple) of (*R*)-**10** computed for the eight low-energy B3LYP/6-31G (d) conformers. The bars represent the rotational strength values of the lowest energy conformer.

(**34**) [36] by comparison of their ^1H NMR and MS data with the literature.

The known compounds isolated in this study are typical fungal metabolites previously reported from the genera *Aspergillus* and *Penicillium* [9–12, 15–36]. The isolated new compounds (**1**, **3**, **9**, and **10**) are biosynthetically related to those known analogues, and thus are suggested to be derived from the fungus.

All isolated compounds (**1**–**34**) were tested for their cytotoxic activity against the mouse lymphoma cell line L5178Y using the microculture tetrazolium method (MTT) (► **Table 4**). The xanthone derivatives sterigmatocystin (**19**), sterigmatin (**20**), and AGI-B4 (**21**) displayed potent cytotoxicity with IC_{50} values of 2.2, 2.3, and 2.0 μM , respectively, even stronger than that of the positive control kahalalide F ($\text{IC}_{50} = 4.3 \mu\text{M}$). *O*-Demethylsterigmatocystin (**18**) showed substantial activity with an IC_{50} value of 5.8 μM . The anthraquinone derivative 8-*O*-methylversicolorin B (**15**) and the alkaloid stephacidin A (**26**) showed only mild activity with IC_{50} values of 21.2 and 16.7 μM , respectively. The remaining compounds revealed no cytotoxic activity.

The antibacterial activity of the isolated compounds was tested against several gram-positive bacteria using the broth microdilution method (► **Table 5**). Versicolorin B (**14**), averufin (**16**) and diorcinols D (**31**), G (**32**), and I (**33**) displayed inhibitory activity with MIC values ranging from 12.5 to 50 μM . Diorcinol G (**32**) exhibited pronounced antibacterial activity against all tested bacterial strains with an MIC value of 12.5 μM . Remarkably, none of the active compounds showed cytotoxicity against the L5178Y

► **Table 4** Cytotoxicity of isolated compounds.

Compound	IC_{50} (μM)
8- <i>O</i> -Methylversicolorin B (15)	21.2
<i>O</i> -Demethylsterigmatocystin (18)	5.8
Sterigmatocystin (19)	2.2
Sterigmatin (20)	2.3
AGI-B4 (21)	2.0
Stephacidin A (26)	16.7
Kahalalide F ^a	4.3
^a Positive control	

cell line, indicating that the observed antibacterial activities are not caused by general toxicity of the respective metabolites.

It is worthy to note that some of these bioactive compounds showed similar activities in the literature. For example, 8-*O*-methylversicolorin B (**15**) showed weak cytotoxic activity against PC-3 cells (human prostate cancer cells) and H460 cells (human lung cancer cells) with IC_{50} values of 19.5 and 27.2 μM , respectively [20], sterigmatocystin (**19**) exhibited significant cytotoxicity on HepG2 cells (human hepatoma cells) at a concentration of 3 μM [37], AGI-B4 (**21**) inhibited VEGF-induced proliferation of HUVECs (human umbilical vein endothelial cells) with an IC_{50} value of 1.4 μM [24], and stephacidin A (**26**) was a selective inhibitor of the testosterone-dependent prostate LNCaP cells with an IC_{50} value of 2.1 μM [29]. Moreover, versicolorin B (**14**) showed antifungal activity against *Fusarium solani*, a pathogenic fungus of *Panax notoginseng*, with an MIC of 16–32 $\mu\text{g}/\text{mL}$ [38]. Averufin (**16**) showed antibacterial activity against *B. subtilis* with an MIC of 8–16 $\mu\text{g}/\text{mL}$ [38]. Diorcinol D (**31**) exhibited antibacterial activity against *Escherichia coli* with an MIC of 8 $\mu\text{g}/\text{mL}$ [39], while diorcinol I (**33**) displayed significant antibacterial activity against *Staphylococcus aureus* with an MIC of 6.25 $\mu\text{g}/\text{mL}$ [40].

In conclusion, the co-cultivation experiment of *A. versicolor* with *B. subtilis* was carried out with the aim of inducing or enhancing secondary metabolite production by the fungus. Comparison of the HPLC chromatograms of the axenic fungal culture and the mixed fungal-bacterial fermentation revealed the upregulation of several metabolites compared to the axenic fungal control (**14**, **16**, and **19**) in addition to the induction of four new metabolites (**1**, **3**, **9**, and **10**) that were not detected in the axenic fungal culture. Sterigmatocystin (**19**) showed a 4.7-fold increase in its amount in the co-culture compared to the axenic culture, while the accumulation of versicolorin B (**14**) and averufin (**16**) was increased by factors of 1.5 and 2.0, respectively. The absolute configuration of compounds **3**, **9**, and **10** was determined by ECD analysis aided by TDDFT-ECD calculations.

Materials and Methods

General experimental procedures

For measurement of optical rotations, a PerkinElmer-241 MC polarimeter was used. NMR spectra were recorded with a Bruker ARX

► **Table 5** Antibacterial activity of isolated compounds (MIC in μM).

Compound	<i>S. aureus</i> ATCC 29213	<i>E. faecalis</i> ATCC 29212	<i>E. faecalis</i> ATCC 51299	<i>E. faecium</i> ATCC 35667	<i>E. faecium</i> ATCC 700221
Versicolorin B (14)	50	> 100	100	100	> 100
Averufin (16)	25	25	25	12.5	12.5
Diorcinol D (31)	25	50	50	12.5	50
Diorcinol G (32)	12.5	12.5	12.5	12.5	12.5
Diorcinol I (33)	50	50	50	25	50
Ciprofloxacin ^a	0.8	–	–	–	–
Moxifloxacin ^a	–	1.2	1.2	5	40

^a Positive control

300 or AVANCE DMX 600 NMR spectrometer. A Finnigan LCQ Deca XP Thermoquest spectrometer was utilized to record low resolution mass spectra. HRESIMS spectra were obtained by a FTHRMS-Orbitrap (Thermo Finnigan) mass spectrometer. A Dionex P580 system equipped with a photodiode array detector (UVD340S) was employed for analytical HPLC analysis, and an analytical HPLC column (Europhere 10 C18, 125 × 4 mm, L × ID) was used. Semipreparative HPLC was accomplished using a Lachrom-Merck Hitachi semipreparative HPLC system with an Europhere 100 C18 (300 × 8 mm) column, pump L7100, and UV detector L7400 at a flow rate of 5 mL/min. For improved resolution of D and L-N-methylphenylalanine residues after Marfey's derivatization, HPLC separation was conducted on an EC 250/4.6 Nucleosil 120–5, C4 (Macherey-Nagel) column. Column chromatographic stationary phases used were Merck MN silica gel 60 M (0.04–0.063 mm) and Sephadex LH-20. The eluted fractions from column chromatographic separations were analyzed by TLC using precoated silica gel 60 F254 plates (Merck). Visualization of spots was done under a UV lamp (254 and 365 nm) or by spaying the plates with anisaldehyde reagent. Distillation of solvents for column chromatography was performed prior to use, while spectral grade solvents were used for spectroscopic measurements. ECD spectra were recorded on a Jasco J-810 spectropolarimeter.

Microbial material

The marine-derived fungus *A. versicolor* (code 8.1.3a) was isolated from the sponge *Agelas oroides*, which was collected at a depth of 10 m in Aliağa-Izmir, Turkey, in December 2014. The sponge was identified by Dr. Mehmet Baki Yökeş (Department of Molecular Biology and Genetics, Faculty of Arts and Sciences, Haliç University, Siracevizler Cd. No: 29 Bomonti, Şişli, Istanbul, Turkey). The bacterial strain used for co-cultivation was the laboratory strain *B. subtilis* 168 trpC2. The fungus *A. versicolor* was identified through DNA amplification and sequencing of the ITS region according to a molecular biological protocol described previously [41]. The obtained sequence data were submitted to GenBank under KY174984. A voucher specimen is stored at the Institute of Pharmaceutical Biology and Biotechnology, Heinrich-Heine-Universität Düsseldorf, Germany.

Co-cultivation experiment of *Aspergillus versicolor* with *Bacillus subtilis*

The mixed fermentation experiment of the fungus *A. versicolor* with *B. subtilis* was carried out on solid rice medium under static conditions in five Erlenmeyer flasks (1 L). The fungal control (axenic *A. versicolor* culture) and bacterial control (axenic *B. subtilis* culture) were also cultivated in five Erlenmeyer flasks each. Autoclaving of the flasks [each containing 60.0 mL of distilled water and 50.0 g of commercially available milk rice (Milch-Reis, ORYZA)] was done prior to inoculation of the fungus and the bacterium. Preparation of *B. subtilis* was accomplished through an overnight culture of the bacterium in lysogeny broth (LB), which was then inoculated to prewarmed LB medium (1 : 20), followed by incubation at 37 °C with shaking at 200 rpm to the mid-exponential growth phase (optical density at 600 nm of 0.2–0.4). The bacterial culture (10 mL) was added to the autoclaved rice medium and then the flasks were incubated for 4 days at 37 °C. *A. versicolor* grown on malt agar was cut into pieces (1 cm × 1 cm). Five pieces were added to each of the flasks that had been previously incubated with *B. subtilis*. The fungal and bacterial controls as well as the co-cultures were left to grow under static conditions at 23 °C. Upon reaching the stationary phase of growth (2 weeks for controls and 4 weeks for co-culture), EtOAc (300 mL) was added to each flask to stop the growth of the cultures, followed by shaking at 150 rpm for 8 h, then keeping them overnight. The flasks were filtered the next day using a Büchner funnel, and the extracts were evaporated under vacuum. The obtained residues were redissolved in MeOH (50 mL), and 30 μL of each resulting extract were injected into the analytical HPLC column.

Extraction and isolation

The crude EtOAc extract (14.3 g, obtained after combining all extracts resulting from the co-cultivation experiment) was fractionated by vacuum liquid chromatography (VLC) on silica gel 60 with a gradient elution solvent system of *n*-hexane-EtOAc (100:0 to 0:100) followed by DCM-MeOH (100:0 to 0:100) to yield 19 fractions (Fr. 1 to Fr. 19).

Fr. 3 (1.6 g) was further chromatographed on a Sephadex LH-20 column using acetone as the mobile phase to yield the pure compound 16 (2.3 mg) in addition to six subfractions (Fr. 3–1 to

Fr. 3–6). Fr. 3–2 (37.7 mg) was separated by semipreparative HPLC using RP-HPLC with a gradient H₂O-MeOH solvent system to afford **33** (3.6 mg), **31** (5.3 mg), and **32** (3.2 mg).

Fr. 4 (3.4 g) was subjected to a Sephadex LH-20 column with acetone as the mobile phase to give seven subfractions (Fr. 4–1 to Fr. 4–7). Part of Fr. 4–3 (100 mg) was chromatographed on a silica gel column with DCM-MeOH (9:1) to afford compound **19** (2.0 mg). Fr. 4–6 (400 mg) was submitted to a Sephadex LH-20 column using acetone as the mobile phase to yield **14** (1 mg) and **4** (4.0 mg).

Fr. 5 (934 mg) was further subjected to a VLC column with an *n*-hexane-EtOAc (100:0 to 0:100) gradient elution solvent system (200 mL for each polarity) to afford 14 subfractions (Fr. 5–1 to Fr. 5–14). Subfraction Fr. 5–7 (30 mg) was purified by semipreparative HPLC with a gradient of H₂O-MeOH to obtain compounds **7** (5.6 mg), **29** (2.1 mg), and **28** (1.0 mg). Subfraction Fr. 5–8 (72 mg) yielded compounds **6** (12.2 mg) and **5** (5.6 mg) after RP-HPLC separation using an H₂O-MeOH gradient solvent system. Fr. 5–9 (50 mg) was subjected to semipreparative HPLC purification with a gradient H₂O-MeOH solvent system to afford compounds **8** (1.7 mg), **24** (3.9 mg), **9** (12.1 mg), **13** (1.7 mg), **3** (1.2 mg), and **15** (3.2 mg).

Fr. 6 (720 mg) was chromatographed on a Sephadex LH-20 column using acetone as the mobile phase to yield six subfractions (Fr. 6–1 to Fr. 6–6). Fr. 6–2 (25 mg) was submitted to RP-HPLC separation using an H₂O-MeOH gradient solvent system to afford compound **23** (1.7 mg). Fr. 6–6 (247.7 mg) was further separated on a Sephadex LH-20 column with acetone as the mobile phase to give five subfractions (Fr. 6–6–1 to Fr. 6–6–5). Fr. 6–6–4 (28 mg) yielded compound **11** (1.4 mg) while Fr. 6–6–5 (31 mg) gave compounds **30** (1.8 mg) and **22** (7.1 mg) after semipreparative HPLC with a gradient H₂O-MeOH solvent system.

Fr. 7 (300 mg) was fractionated on a Sephadex LH-20 column with acetone as the mobile phase to afford seven subfractions (Fr. 7–1 to Fr. 7–7). Fr. 7–2 (34.1 mg), Fr. 7–3 (15.8 mg), Fr. 7–5 (10.8 mg), and Fr. 7–7 (28.1 mg) were purified by semipreparative HPLC with a gradient H₂O-MeOH solvent system to obtain compounds **34** (8.9 mg), **21** (5.5 mg), **10** (3.2 mg), and **12** (3.1 mg), respectively.

Fr. 10 (99.2 mg) was chromatographed on a Sephadex LH-20 column using MeOH as the mobile phase to yield three subfractions (Fr. 10–1 to Fr. 10–3). Fr. 10–1 (32.9 mg) was purified by RP-HPLC separation using an H₂O-MeOH gradient solvent system to obtain compound **2** (4.5 mg).

Fr. 11 (2.9 g) was subjected to a VLC column using DCM-MeOH (100:0 to 0:100) with 300 mL eluting volume for each step to afford 13 subfractions (Fr. 11–1 to Fr. 11–13). Subfraction Fr. 11–4 (200 mg) was then separated on a Sephadex LH-20 column using acetone as the mobile phase to give four subfractions (Fr. 11–4–1 to Fr. 11–4–4). Fr. 11–4–2 (40 mg) afforded compounds **1** (2.5 mg) and **25** (2.4 mg) after purification by semipreparative HPLC with a gradient H₂O-MeOH solvent system. In addition, Fr. 11–4–3 (60 mg) was subjected to RP-HPLC separation using an H₂O-MeOH gradient solvent system to yield compounds **26** (5.8 mg) and **27** (2.2 mg).

Fr. 12 (499.5 mg) was chromatographed on a Sephadex LH-20 column using MeOH as the mobile phase to obtain six subfrac-

tions (Fr. 12–1 to Fr. 12–6). Fr. 12–5 (27.2 mg) was purified by RP-HPLC separation using an H₂O-MeOH gradient solvent system to yield compound **17** (3.1 mg).

Fr. 15 (132.1 mg) was separated on a Sephadex LH-20 column using MeOH as the mobile phase to obtain four subfractions (Fr. 15–1 to Fr. 15–4). Compounds **18** (0.9 mg) and **20** (0.7 mg) were obtained from Fr. 15–2 (39 mg) after semipreparative HPLC purification using a gradient H₂O-MeOH elution system.

Cotteslosin C (**1**): dark amorphous solid; $[\alpha]_D^{23} - 89$ (c 0.11, MeOH); UV (MeOH): λ_{\max} 277, 203 nm; ¹H and ¹³C NMR data see ► **Table 1**; HRESIMS $[M + H]^+ m/z$ 620.3442 (calcd. for C₃₄H₄₆N₅O₆, 620.3443).

22-Epi-aflaquinolone B (**3**): yellow amorphous powder; $[\alpha]_D^{22} - 15$ (c 0.14, MeOH); UV (MeOH) λ_{\max} 324, 278 and 212 nm; ECD (MeOH, λ [nm] ($\Delta\epsilon$), c 0.114 mM): 322 sh (+2.32), 281 (+6.16), 253 (–13.73), 220 (+13.44), 201 sh (+6.86); ¹H and ¹³C NMR data see ► **Table 2**; HRESIMS $[M + H]^+ m/z$ 438.2271 (calcd. for C₂₆H₃₂NO₅, 438.2275), $[M + Na]^+ m/z$ 460.2092 (calcd. for C₂₆H₃₁NNaO₅, 460.2094).

Isoversicolorin B (**9**): orange red amorphous powder; $[\alpha]_D^{23} + 43$ (c 0.2, MeOH); UV (MeOH) λ_{\max} 437, 285, and 223 nm; ECD (MeCN, λ [nm] ($\Delta\epsilon$), c 0.147 mM): 419 sh (+0.43), 363 (+1.46), 308 (–2.10), 280 (+3.87), 256 (–0.39), 238 sh (+0.20), 231 (+0.44), 205 sh (–3.07); ¹H and ¹³C NMR data see ► **Table 3**; HRESIMS $[M + H]^+ m/z$ 341.0654 (calcd. for C₁₈H₁₃O₇, 341.0656).

6,8-O-Dimethylbipolarin (**10**): orange solid; $[\alpha]_D^{23} - 57$ (c 0.38, MeOH); UV (MeOH) λ_{\max} 440, 287, and 223 nm; ECD (MeOH, λ [nm] ($\Delta\epsilon$), c 0.114 mM): 386 (–0.62), 311 (+1.04), 282 (–0.89), 260 (+0.04), 231 (–1.63), 220 sh (+0.32); ¹H and ¹³C NMR data see ► **Table 3**; HRESIMS $[M + H]^+ m/z$ 371.1125 (calcd. for C₂₀H₁₉O₇, 371.1125).

Marfey's analysis

Compound **1** (0.5 mg) was subjected to acid hydrolysis by adding 1 mL of 6 N HCl, followed by heating at 110 °C for 24 h. The resulting acid hydrolysate solution was concentrated under reduced pressure with the successive addition of H₂O (5 mL each) to guarantee removal of HCl. Derivatization of the resulting amino acids was done by treating 25 μ L of the hydrolysate with 50 μ L of FDNPL [1% *N*-(5-fluoro-2,4-dinitrophenyl)-L-leucinamide in acetone] and 10 μ L of 1 M NaHCO₃, followed by heating the mixture for 1 h at 40 °C on a hot plate with frequent mixing. The reaction mixture was then allowed to cool, followed by the addition of 5 μ L of 2 N HCl to the solution and then concentration to dryness. The derivatized amino acids were submitted to analytical HPLC after dissolving the mixture in 1 mL of MeOH. The standard amino acids (L- and D-forms) were derivatized following the same procedure. Comparison of the retention times of the derivatized amino acids with the derivatized standard amino acids was performed using HPLC (C18) analysis (a gradient of MeOH and 0.1% HCOOH in H₂O): 0 min (10% MeOH); 5 min (10% MeOH); 35 min (100% MeOH); 45 min (100% MeOH); 50 min (10% MeOH); 25 °C, 1 mL/min). A C4 analytical HPLC was employed for better resolution of the derivatized D and L-*N*-Me-phenylalanine residues (C-4 column HPLC separation using a gradient of MeOH and 0.1% HCOOH in H₂O): 0 min (15% MeOH); 2 min (15% MeOH); 180 min (65%

MeOH); 181 min (100% MeOH); 185 min (100% MeOH); 186 min (15% MeOH); 190 min (15% MeOH); 30 °C, 1 mL/min.

Cytotoxicity assay

All isolated compounds were tested for their cytotoxic activity against the murine lymphoma cell line L5178Y (Sigma) using the MTT method. Briefly, cells were placed on a 96-well plate with 3000 cells/mL. The cells were allowed to attach for 24 h and then were treated with different concentrations of the compounds starting with 30 μ M for 72 h. Usually 4 to 7 concentrations of the respective compounds fall into the dose-response range between 20 to 90% inhibition. Ten parallel experiments were performed per concentration point. The mathematical, nonlinear regression (4-parameter model) was applied. The IC₅₀ values were calculated from a sigmoidal dose-response curve using GraphPad Prism software. The depsipeptide kahalalide F (purity 97%) obtained from *Elysia grandifolia* [42] was used as a positive control, while media containing 0.1% ethylene glycol monomethyl ether (used for dissolving the compounds in the cell culture media) were used as a negative control.

Antibacterial assay

Antibacterial activity of the compounds was analyzed against several gram-positive bacteria using the broth microdilution method. Compounds were predissolved in DMSO and added to the broth. The resulting final DMSO concentration in the assay was 0.1%. The direct colony suspension method was employed for preparation of the inoculum, and MIC for each strain was determined according to the recommendations of the Clinical and Laboratory Standards Institute [43]. Ciprofloxacin and moxifloxacin (analytical standard; Sigma-Aldrich) were used as positive controls.

Computational section

Mixed torsional/low-frequency mode conformational searches were carried out by means of Macromodel 10.8.011 software by using the MMFF with an implicit solvent model for CHCl₃ [44]. Geometry reoptimizations were carried out at the B3LYP/631G(d) level *in vacuo* and CAM-B3LYP/TZVP levels with the PCM (polarizable continuum model) solvent model for MeCN or MeOH [45, 46]. Time-dependent density functional theory – ECD calculations were run with various functionals (B3LYP, BH&HLYP, CAM-B3LYP, and PBE0) and the TZVP basis set as implemented in the Gaussian 09 package with the same or no solvent model as in the preceding DFT optimization step [47]. ECD spectra were generated as sums of Gaussians with 3000 and 2100 cm⁻¹ half-height widths using dipole-velocity-computed rotational strength values [48]. Boltzmann distributions were estimated from the ZPVE-corrected B3LYP energies in the gas-phase calculations and from the CAM-B3LYP energies in the solvated ones. The MOLEKEL software package was used for visualization of the results [49].

Supporting information

HRESIMS and NMR spectra of compounds **1**, **3**, **9**, and **10**, ECD calculations for compound **10**, HPLC chromatograms of EtOAc extracts from co-culture experiments and Marfey's analysis for compound **1** are available as Supporting Information.

Acknowledgements

Financial support by the DFG (GRK 2158) and by the Manchot Foundation to P. P. is gratefully acknowledged. T. K. and A. M. thank the National Research, Development and Innovation Office (NKFI K120181 and PD121020) for financial support and the Governmental Information-Technology Development Agency (KIFÜ) for CPU time.

Conflict of Interest

The authors declare no conflict of interest.

References

- [1] Rateb ME, Ebel R. Secondary metabolites of fungi from marine habitats. *Nat Prod Rep* 2011; 28: 290–344
- [2] Almeida C, El Maddah F, Kehraus S, Schnakenburg G, König GM. Endolides A and B, vasopressin and serotonin-receptor interacting N-methylated peptides from the sponge-derived fungus *Stachylidium* sp. *Org Lett* 2016; 18: 528–531
- [3] Liu J, Gu B, Yang L, Yang F, Lin H. New anti-inflammatory cyclopeptides from a sponge-derived fungus *Aspergillus violaceofuscus*. *Front Chem* 2018; 6: 226
- [4] Brakhage AA, Schroeckh V. Fungal secondary metabolites – strategies to activate silent gene clusters. *Fungal Genet Biol* 2011; 48: 15–22
- [5] Marmann A, Aly A, Lin W, Wang B, Proksch P. Co-cultivation – a powerful emerging tool for enhancing the chemical diversity of microorganisms. *Mar Drugs* 2014; 12: 1043–1065
- [6] Liu S, Dai H, Heering C, Janiak C, Lin W, Liu Z, Proksch P. Inducing new secondary metabolites through co-cultivation of the fungus *Pestalotiopsis* sp. with the bacterium *Bacillus subtilis*. *Tetrahedron Lett* 2017; 58: 257–261
- [7] Ebrahim W, El-Neketi M, Lewald LI, Orfali RS, Lin W, Rehberg N, Kalscheuer R, Daletos G, Proksch P. Metabolites from the fungal endophyte *Aspergillus austroafricanus* in axenic culture and in fungal-bacterial mixed cultures. *J Nat Prod* 2016; 79: 914–922
- [8] Abdelwahab MF, Kurtán T, Mándi A, Müller WEG, Fouad MA, Kamel MS, Liu Z, Ebrahim W, Daletos G, Proksch P. Induced secondary metabolites from the endophytic fungus *Aspergillus versicolor* through bacterial co-culture and OSMAC approaches. *Tetrahedron Lett* 2018; 59: 2647–2652
- [9] Fremlin LJ, Piggott AM, Lacey E, Capon RJ. Cottoquinazoline A and cotteslosins A and B, metabolites from an Australian marine-derived strain of *Aspergillus versicolor*. *J Nat Prod* 2009; 72: 666–670
- [10] Neff SA, Lee SU, Asami Y, Ahn JS, Oh H, Baltrusaitis J, Gloer JB, Wicklow DT. Aflaquinolones A–G: secondary metabolites from marine and fungicolous isolates of *Aspergillus* spp. *J Nat Prod* 2012; 75: 464–472
- [11] Hamasaki T, Hatsuda Y, Terashima N, Renbutsu M. The structure of two new metabolites of *Aspergillus versicolor*. *Agric Biol Chem* 1965; 29: 166–167
- [12] Jakšić D, Puel O, Canlet C, Kopjar N, Kosalec I, Klarić MŠ. Cytotoxicity and genotoxicity of versicolorins and 5-methoxyterigmatocystin in A549 cells. *Arch Toxicol* 2012; 86: 1583–1591
- [13] Mándi A, Mudianta IW, Kurtán T, Garson MJ. Absolute configuration and conformational study of psammaphysins A and B from the balinese marine sponge *Aplysinella strongylata*. *J Nat Prod* 2015; 78: 2051–2056
- [14] Superchi S, Scafato P, Górecki M, Pescitelli G. Absolute configuration determination by quantum mechanical calculation of chiroptical spectra: basics and applications to fungal metabolites. *Curr Med Chem* 2017; 25: 287–320
- [15] Castonguay A, Brassard P. C-Alkylation of 1,3-dihydroxyanthraquinones. Total syntheses of (±)-averufin and (±)-bipolarin. *Can J Chem* 1977; 55: 1324–1332

- [16] Hodge RP, Harris CM, Harris TM. Verrucofortine, a major metabolite of *Penicillium verrucosum* var. *cyclopium*, the fungus that produces the mycotoxin verrucosidin. *J Nat Prod* 1988; 51: 66–73
- [17] Pan C, Shi Y, Chen X, Chen CTA, Tao X, Wu B. New compounds from a hydrothermal vent crab-associated fungus *Aspergillus versicolor* XZ-4. *Org Biomol Chem* 2017; 15: 1155–1163
- [18] Lee YM, Li H, Hong J, Cho HY, Bae KS, Kim MA, Kim DK, Jung JH. Bioactive metabolites from the sponge-derived fungus *Aspergillus versicolor*. *Arch Pharmacol Res* 2010; 33: 231–235
- [19] Steyn PS, Vlegaar R, Wessels PL, Cole RJ. Structure and carbon-13 nuclear magnetic resonance assignments of versiconal acetate, versiconol acetate, and versiconol, metabolites from cultures of *Aspergillus parasiticus* treated with dichlorvos. *J Chem Soc Perkin Trans* 1979; 1: 451–459
- [20] Dou Y, Wang X, Jiang D, Wang H, Jiao Y, Lou H, Wang X. Metabolites from *Aspergillus versicolor*, an endolichenic fungus from the lichen *Lobaria retigera*. *Drug Discoveries Ther* 2014; 8: 84–88
- [21] Yamazaki M, Satoh Y, Maebayashi Y, Horie Y. Monoamine oxidase inhibitors from a fungus: *Emericella navahoensis*. *Chem Pharm Bull* 1988; 36: 670–675
- [22] Kikuchi N, Teshiba M, Tsutsumi T, Fudou R, Nagasawa H, Sakuda S. Endocrocin and its derivatives from the Japanese mealybug *Planococcus kraunhiae*. *Biosci Biotechnol Biochem* 2011; 75: 764–767
- [23] Hamasaki T, Matsui K, Isono K, Hatsuda Y. A new metabolite from *Aspergillus versicolor*. *Agric Biol Chem* 1973; 37: 1769–1770
- [24] Kim HS, Park IY, Park YJ, Lee JH, Hong YS, Lee JJ. A novel dihydroxanthone, AGI-B4 with inhibition of VEGF-induced endothelial cell growth. *J Antibiot* 2002; 55: 669–672
- [25] Hamasaki T, Sato Y, Hatsuda Y. Structure of sydowinin A, sydowinin B, and sydowinol, metabolites from *Aspergillus sydowi*. *Agric Biol Chem* 1975; 39: 2341–2345
- [26] Kato H, Yoshida T, Tokue T, Nojiri Y, Hirota H, Ohta T, Williams RM, Tsukamoto S. Notoamides A–D: prenylated indole alkaloids isolated from a marine derived fungus, *Aspergillus* sp. *Angew Chem Int Ed Engl* 2007; 119: 2304–2306
- [27] Chang YW, Yuan CM, Zhang J, Liu S, Cao P, Hua HM, Di YT, Hao XJ. Speramides A–B, two new prenylated indole alkaloids from the freshwater-derived fungus *Aspergillus ochraceus* KM007. *Tetrahedron Lett* 2016; 57: 4952–4955
- [28] Tsukamoto S, Kato H, Greshock TJ, Hirota H, Ohta T, Williams RM. Isolation of notoamide E, a key precursor in the biosynthesis of prenylated indole alkaloids in a marine-derived fungus, *Aspergillus* sp. *J Am Chem Soc* 2009; 131: 3834–3835
- [29] Qian-Cutrone J, Huang S, Shu YZ, Vyas D, Fairchild C, Menendez A, Krampitz K, Dalterio R, Klohr SE, Gao Q. Stephacidin A and B: two structurally novel, selective inhibitors of the testosterone-dependent prostate LNCaP cells. *J Am Chem Soc* 2002; 124: 14556–14557
- [30] Tsukamoto S, Umaoka H, Yoshikawa K, Ikeda T, Hirota H. Notoamide O, a structurally unprecedented prenylated indole alkaloid, and notoamides P–R from a marine-derived fungus, *Aspergillus* sp. *J Nat Prod* 2010; 73: 1438–1440
- [31] Lee SU, Asami Y, Lee D, Jang JH, Ahn JS, Oh H. Protuboxepins A and B and protubonines A and B from the marine-derived fungus *Aspergillus* sp. SF-5044. *J Nat Prod* 2011; 74: 1284–1287
- [32] Ishikawa N, Tanaka H, Koyama F, Noguchi H, Wang CC, Hotta K, Watanabe K. Non-Heme dioxygenase catalyzes atypical oxidations of 6,7-bicyclic systems to form the 6,6-quinolone core of viridicatin-type fungal alkaloids. *Angew Chem Int Ed Engl* 2014; 126: 13094–13098
- [33] Trisuwan K, Rukachaisirikul V, Borwornwiriyanon K, Phongpaichit S, Sakayaroj J. Benzopyranone, benzophenone, and xanthone derivatives from the soil fungus *Penicillium citrinum* PSU-RSPG95. *Tetrahedron Lett* 2014; 55: 1336–1338
- [34] Gao H, Zhou L, Cai S, Zhang G, Zhu T, Gu Q, Li D. Diorcinols B–E, new prenylated diphenyl ethers from the marine-derived fungus *Aspergillus versicolor* ZLN-60. *J Antibiot* 2013; 66: 539–542
- [35] Li XB, Zhou YH, Zhu RX, Chang WQ, Yuan HQ, Gao W, Zhang LL, Zhao ZT, Lou HX. Identification and biological evaluation of secondary metabolites from the endolichenic fungus *Aspergillus versicolor*. *Chem Biodivers* 2015; 12: 575–592
- [36] Sassa T, Takemura T, Ikeda M, Miura Y. Structure of radiclonic acid, a new plant growth-regulator produced by a fungus. *Tetrahedron Lett* 1973; 14: 2333–2334
- [37] Gao W, Jiang L, Ge L, Chen M, Geng C, Yang G, Li Q, Ji F, Yan Q, Zou Y, Zhong L, Liu X. Sterigmatocystin-induced oxidative DNA damage in human liver-derived cell line through lysosomal damage. *Toxicol In Vitro* 2015; 29: 1–7
- [38] Liu K, Zheng Y, Miao C, Xiong Z, Xu L, Guan H, Yang Y, Zhao L. The anti-fungal metabolites obtained from the rhizospheric *Aspergillus* sp. YIM PH30001 against pathogenic fungi of *Panax notoginseng*. *Nat Prod Res* 2014; 28: 2334–2337
- [39] Li ZX, Wang XF, Ren GW, Yuan XL, Deng N, Ji GX, Li W, Zhang P. Prenylated diphenyl ethers from the marine algal-derived endophytic fungus *Aspergillus tennesseensis*. *Molecules* 2018; 23: E2368
- [40] Xu X, Yang H, Xu H, Yin L, Chen Z, Shen H. Diphenyl ethers from a marine-derived isolate of *Aspergillus* sp. CUGB-F046. *Nat Prod Res* 2018; 32: 821–825
- [41] Kjer J, Debbab A, Aly AH, Proksch P. Methods for isolation of marine-derived endophytic fungi and their bioactive secondary products. *Nat Protoc* 2010; 5: 479–490
- [42] Ashour M, Edrada R, Ebel R, Wray V, Wätjen W, Padmakumar K, Müller WEG, Lin WH, Proksch P. Kahalalide derivatives from the Indian sacoglossan mollusk *Elysia grandifolia*. *J Nat Prod* 2006; 69: 1547–1553
- [43] Clinical and Laboratory Standards Institute. Methods for Dilution antimicrobial Susceptibility Tests for Bacteria that grow aerobically. Approved Standard – Ninth Ed. CLSI Document M07-A9. Wayne, PA: Clinical and Laboratory Standards Institute; 2012
- [44] MacroModel. New York: Schrödinger LLC; 2015. Available at <https://www.schrodinger.com/macromodel>. Accessed January 23, 2018
- [45] Yanai T, Tew DP, Handy NC. A new hybrid exchange – correlation functional using the Coulomb-attenuating method (CAM-B3LYP). *Chem Phys Lett* 2004; 393: 51–57
- [46] Pescitelli G, Bruhn T. Good computational practice in the assignment of absolute configurations by TDDFT calculations of ECD spectra. *Chirality* 2016; 28: 466–474
- [47] Frisch MJ, Trucks GW, Schlegel HB, Scuseria GE, Robb MA, Cheeseman JR, Scalmani G, Barone V, Mennucci B, Petersson GA, Nakatsuji H, Caricato M, Li X, Hratchian HP, Izmaylov AF, Bloino J, Zheng G, Sonnenberg JL, Hada M, Ehara M, Toyota K, Fukuda R, Hasegawa J, Ishida M, Nakajima T, Honda Y, Kitao O, Nakai H, Vreven T, Montgomery JA jr., Peralta JE, Ogliaro F, Bearpark M, Heyd JJ, Brothers E, Kudin KN, Staroverov VN, Kobayashi R, Normand J, Raghavachari K, Rendell A, Burant JC, Iyengar SS, Tomasi J, Cossi M, Rega N, Millam JM, Klene M, Knox JE, Cross JB, Bakken V, Adamo C, Jaramillo J, Gomperts R, Stratmann RE, Yazyev O, Austin AJ, Cammi R, Pomelli C, Ochterski JW, Martin RL, Morokuma K, Zakrzewski VG, Voth GA, Salvador P, Dannenberg JJ, Dapprich S, Daniels AD, Farkas Ö, Foresman JB, Ortiz JV, Cioslowski J, Fox DJ. Gaussian 09, Revision B.01. Wallingford, CT: Gaussian, Inc.; 2010
- [48] Stephens PJ, Harada N. ECD cotton effect approximated by the Gaussian curve and other methods. *Chirality* 2010; 22: 229–233
- [49] Varetto U. MOLEKEL 5.4. Manno, Switzerland: Swiss National Supercomputing Centre; 2009